Author(s): David E. Cooper, Mark Stanford, Kevin A. Kibble, Gregory J. Gibbons

Article Title: Additive Manufacturing for product improvement at Red Bull Technology

Year of publication: 2012

Link to published article:
http://link.aps.org/doi/10.1016/j.matdes.2012.05.017


Technical report

# Additive Manufacturing for Product Improvement at Red Bull Technology

David E. Cooper, Mark Stanford, Kevin A. Kibble, Gregory J. Gibbons

| | |
|---|---|
| PII: | S0261-3069(12)00318-4 |
| DOI: | http://dx.doi.org/10.1016/j.matdes.2012.05.017 |
| Reference: | JMAD 4530 |

| | |
|---|---|
| To appear in: | *Materials and Design* |

| | |
|---|---|
| Received Date: | 30 January 2012 |
| Accepted Date: | 5 May 2012 |

Please cite this article as: Cooper, D.E., Stanford, M., Kibble, K.A., Gibbons, G.J., Additive Manufacturing for Product Improvement at Red Bull Technology, *Materials and Design* (2012), doi: http://dx.doi.org/10.1016/j.matdes.2012.05.017

**Title:**
Additive Manufacturing for Product Improvement at Red Bull Technology

**Author Names and affiliations:**
Mr David E. Cooper [a]
Dr Mark Stanford [b]
Dr Kevin A. Kibble [c]
Dr Gregory J. Gibbons [d]

a WMG, International Manufacturing Centre, University of Warwick, Coventry, CV4 7AL, UK, d.e.cooper@warwick.ac.uk.
b School of Engineering and the Built Environment, University of Wolverhampton, Telford, Shropshire, TF2 9NT, UK, m.stanford@wlv.ac.uk.
c School of Engineering and the Built Environment, University of Wolverhampton, Telford, Shropshire, TF2 9NT, UK, k.a.kibble@wlv.ac.uk
d WMG, International Manufacturing Centre, University of Warwick, Coventry, CV4 7AL, UK, g.j.gibbons@warwick.ac.uk.

**Corresponding Author**
Dr Gregory J. Gibbons
WMG,
International Manufacturing Centre,
University of Warwick,
Coventry,
West Midlands,
CV4 7AL, UK.
g.j.gibbons@warwick.ac.uk.
Phone: +44 24 7652 2524
Fax: +44 24 7657 5366

**Abstract**
In Formula 1 racing, there is a strong motive for reducing component weight and thereby improving efficiency. This paper demonstrates the advantages Additive Manufacturing brings to the production of hydraulic components. The Direct Metal Laser Sintering (DMLS) production technique enables weight reductions to be attained by its geometric design freedom coupled with this material's attributes. The use of EOS Titanium Ti64 material for hydraulic components has been assessed by a hydraulic soak test at 25 MPa and no significant losses or failure occurred. The benefits to the efficiency of hydraulic flow have been measured using Particle Image Velocimetry (PIV) and the use of DMLS manufactured geometry has improved flow characteristics by 250% over that of the currently used techniques of manufacturing channels and bores.

**Keywords**
A. Non-ferrous metals and alloys
C. Lasers
C. Sintering

## 1. Introduction

The process of Direct Metal Laser Sintering (DMLS) is one of a number of Additive Manufacturing (AM) processes in which 3D components or parts are constructed by the layer-additive addition of material directly from CAD data. AM removes the shackles of reliance on mould tools, and offers the potential for virtually unlimited complexity and design freedom, allowing the manufacture of complex internal structure and freeform geometry. In DMLS (EOS GmbH), a high power laser is used to melt a powder feed-stock to form fully dense metallic parts.

The use of DMLS gives design and manufacturing freedom without the restrictions of traditional machining processes, bringing with it the benefit of lighter components, and, for hydraulic components, an ability to enhance internal flow paths, thus greatly improving the flow characteristics and ultimately resulting in less energy demanded of the engine by the hydraulic systems. The additive layer process of DMLS in this respect could be advantageous to many component designs throughout the Formula 1 racing environment. Although current F1 race teams are capable of producing a car with a mass less than 640 kg (the FIA minimum [1]), the advantageous weight reduction which is to be gained utilising DMLS would then allow the designers to apportion the mass gained in other areas or components of the car, to help improve reliability of other components. Currently, most hydraulic components are designed for and manufactured mainly from aluminium billet by 5-axis CNC machining and other processes typically including drilling and spark erosion.

DMLS technology has moved the concept of Rapid Prototyping [2-4] into the realm of real time manufacturing of metal components which have been proven for use within some of the most demanding environments and applications to be found [5-7]. One attractive aspect of DMLS is that design and production costs do not rise exponentially with the potential complexity of the design [8].

Engineers have been hesitant in embracing DMLS technology having reservations about the material's mechanical integrity, density and the repeatability of the DMLS process [9]. These aspects will be reviewed and discussed in this paper.

Red Bull Technology identified a desire to explore the application of the DMLS process in the design and manufacture of their hydraulic manifolds. The initial research focused on the metallurgical and mechanical aspects of the material, and then to investigate whether the DMLS process could be realistically relied upon to deliver both significantly lighter, and hydraulically more efficient manifolds than those currently produced by traditional methods, without compromising their reliability and safety.

## 2. Experimental Method

### *2.1. Design and Manufacture*

In order to evaluate the use of DMLS for the manufacture of hydraulic components, samples suitable for pressure testing were required. Several test pipes were designed with wall thicknesses ranging from 0.5mm up to 2mm, with different cross-sections (circular, elliptical and hexagonal).

The test pieces (Fig. 1) were produced using the EOSINT M270 machine (EOS GmbH, Krailling, Germany) and were manufactured from EOS Titanium Ti64 powder (Ti 6Al 4V), by the University of Wolverhampton, using the latest standard build parameters. The parts were orientated as horizontal tubes and were stress relieved at 790$^{o}$C for 90 minutes and allowed to cool naturally in the furnace before being removed from the titanium base plate by

Wire Electrical Discharge Machining (Wire EDM). The remaining support structure was removed by CNC milling. In order to pressure test the samples, a thread and a smooth surface finish suitable for a Dowty seal at a pressure of 25MPa was applied to the boss at each end using a CNC Lathe. The machinability of the material was found to be good, with standard carbide replacement tooling employed.

Fig. 1. DMLS parts both pre (a) and post (b) machined.

*2.2. Pressure Testing*

Pressure tests were undertaken to establish whether or not the material could withstand the operating pressure of the race car's hydraulic systems without mechanical failure or losses in pressure due to porosity. A test rig (Fig. 2) was constructed, which comprised a twin walled steel enclosure which served both as an oven (monitored and controlled by two thermocouples) and also as a safety chamber in case of a catastrophic failure. Incorporated in the hydraulic system was an electronic pressure sensor and the system was pressurised by a double acting hand operated hydraulic pump. The system design was deliberately minimalistic with regards to components and connections to reduce potential pressure leaks.

Fig. 2. Pressure test rig, twin walled safety enclosure, pressure sensor & valve.

The pressure test employed followed an internal standard within Red Bull Racing. The standard is based on BS 2624, which covers pressure impulse testing of aerospace hydraulic system components [10]. The test methodology differs from the standard in that a operating pressure of 110% at operating temperature was employed in a static test, rather than a pressure of 115% at operating temperature in dynamic test (1Hz). Each test piece was connected to the hydraulic rig, and the oven temperature was raised to 140$^{o}$C, this being the maximum operating temperature of the hydraulic fluid, at a rate of 10$^{o}$C/min. When at operating temperature, the pressure, logged through the pressure sensor, was incrementally raised by 2.5MPa, held at each level for a period of 2 minutes, to a final pressure of 25MPa, this being 3MPa above the application operating pressure. Once proven at 25MPa, the pressure was then reduced to 24MPa (10% above operating criteria) and left for an extended "soak" test of 20 minutes to observe pressure losses. The thinnest wall, 0.5mm, samples were also given an extended test of an additional 30 minutes at 24MPa.

*2.3. Flow Visualisation*

Particle Image Velocimetry (PIV) observes and quantifies a fluid flow within a plane, and is often utilised in the automotive industry for examining internal flows [11, 12]. A Flow Visualisation study was conducted using PIV, having a twofold purpose: primarily to assess the benefits to the flow, but also to demonstrate the geometric freedom layer manufacturing can provide in producing internal complex flow passages.

The comparative assessments were made by using clear test pieces, manufactured using stereolithography (SLA 5000, 3D Systems Corp, Rock Hill, USA) in XC11122 resin (DSM Functional Materials, Elgin, USA). One of the test pieces formed within the SLA material emulated an historic example, the second being designed for DMLS.

A pumped closed system was filled with a fluid which matched the refractive index of the SLA material (n=1.512 [13]) so as to render the flow passage boundaries translucent, removing refractive effects and improving image clarity, thus enabling the camera to image the glass particles. The liquid identified as a match was a Silicone Oil (IMCD UK Ltd, Sutton, UK) (n= 1.511).

The passage of glass particles in the fluid was recorded using a high speed camera. The images were then processed frame-by-frame using the DaVis software suite (LaVision GmbH, Goettingen, Germany), correlating individual particles in one frame with the next to obtain a vector for its movement. Using an interrogation window with multiple passes, and with a decreasing window size each pass, a best guess window shift from pass to pass and a more accurate correlation on the final pass was obtained. [14]

### *2.4. Surface Roughness Measurement*

In order to assess the surface roughness of components produced using the EOSINT M270, a Wyko NT 9300 non-contact interferometer (Bruker AXS, Swavesey, UK) was used to measure the surface at multiple points. The system was used in Vertical Scanning mode, with a measurement area of 611.4 x 465.3mm. The measurement process system conformed to the BS EN ISO 25178 standard [15].

### *2.5. Dimensional Accuracy Measurement*

To assess any changes in their geometry and alignment, a dimensional accuracy measurement was made of each sample after building and after pressure testing. Measurement was made using a portable measuring arm (Faro Titanium arm - Faro Technologies UK Ltd, Coventry, UK). The alignment of planes parallel and perpendicular to the sample's axis were probed (±0.1mm), allowing axial bending and torsional rotation of the samples to be assessed. The measurement process system conformed to the BS EN ISO 10360 standard [16].

### *2.6. Microhardness Testing*

Samples cut from representative sample of each production batch were hot-mounted and polished to 1μm. A microhardness measurement was made using a Buehler OmniMet MHT microhardness tester (Buehler UK Ltd, Coventry, UK) to obtain the Vickers hardness number. These measurements were used to observe the consistency of production and also as baseline data for further research on the effects of finishing processes. The microhardness testing complied with the BS EN ISO 14577-1 standard [17].

### *2.7. Porosity Measurement*

Samples were hot mounted and polished to 3μm, and hydrofluoric acid etched. Optical microscopic images were taken (Olympus Lext confocal microscope, Olympus Microscopy, Southend-On-Sea, UK). Porosity levels were measured using image analysis software (a4i, aquinto AG, Berlin, Germany). There is to the best knowledge of the author, no available test standard for determining the porosity of laser sintered materials. It is envisaged that these are to be enshrined in the ASTM standards being developed by the F42-1 development committee. The author took ASTM E2109 – 01 [18] as a test methodology, which covers areal porosity measurement in thermal sprayed coatings, which are derived from a powder feedstock, and deemed approporiate for the sintered materials.

## 3. Results and Discussion

### *3.1. Pressure Testing*

All of the samples (wall thicknesses 0.5 mm – 2 mm) survived without failure during the test sequence, despite the high pressures applied to them. For each sample, a consistent pressure drop (~3%) was observed during the first 5-6 minutes during pressure application. In the proceeding 20 minute test (at 24MPa), the pressure remained constant. The initial loss was attributed as inherent in the system, as it was observed across all samples. No statistically significant pressure loss was observed for the 30 minutes extended pressure test for the 0.5 mm wall thickness samples.

*3.2. Flow Visualisation*

Fig. 3 and Fig. 4 show the average vector field across 500 frames for two cases of traditional and AM geometries. The SLA test samples used for the flow analysis are also provided for reference. As expected, there are areas of recirculation in the traditional geometry with abrupt changes in direction reducing the flow velocity. This condition is associated with overlapping hole intersections "dead-ends" in the traditional design, an inevitability of the manufacturing process where bores have been blocked with Lee plugs.

Fig. 3. Vector fields and test samples for traditional and AM geometry 1.

Fig. 4. Vector fields and test samples for traditional and AM geometry 2.

The measurements of the maximum fluid velocity at the exit and at a centre point of the flow path for the traditional and e-manufactured geometries are given in Table. 1.

Table. 1. Fluid flow measurements for traditional and e-manufactured geometries at centre and end points of the flow path.

The increase in fluid flow velocity is significant (up to 250% for end point and 160% for the centre point). The ability of ALM to produce complex internal flow channels has often been utilised to improve surface cooling [19]. For this application however, the faster flow can be attributed directly to the kinetic energy contained within the fluid. Reduced energy losses during transport will allow more energy to be available at its destination, resulting in a lower energy input from the engine to achieve the same operating effect.

*3.3. Surface Roughness Results*

Table. 2 gives surface roughness measured at different positions around the test piece, showing significant finish variations dependent upon the location of the face relative to the build orientation. These were consistent over all the test pieces. The upper surface shows the best quality of finish, whereas the $R_a$ of angled faces was compromised by the stair-stepping effect symptomatic of AM processing, with the downward facing surface found to be rougher than the upper facing surface. The roughest surfaces were those where supporting structures were required for the DMLS build process (in this case to support the tubular section). There may exist therefore a need for post-process finishing to some areas.

Table. 2. Surface roughness measurements for the DMLS samples.

Good surface finishes are particularly important to hydraulic applications, with union surfaces typically requiring machining to 0.4μm [4]. Also, smooth surface finishes on internal bores serve to aid in improving flow efficiency, and thus post-processing to improve the finish of internals may be necessary. While the need for design rules and improved surface finish for ALM components have been previously identified [20, 21], it would be idealistic to hope for a process which did not require some post-processing in this demanding application, however by characterising the surface finish generated at different build orientations, designers can optimise their geometry for the minimum of essential post processing if build orientation is properly considered during design.

### *3.4. Dimensional Accuracy Measurement*

Table. 3 gives the torsional and axial alignments of the samples, measured before and after pressure testing.

Table. 3. Torsional and axial alignments for the DMLS samples.

Dimensional measurements prior to pressure testing show a slight distortion in the samples. The highest deviations are seen in the thinnest wall section components, most likely from stresses created during the build process due to the large differences in cross-sectional area, as has been reported in previous studies [22]. Measurement after pressure and temperature testing showed a small increase in torsional and axial deformation, attributable to the torque and forces applied when fitting samples to the test rig rather than to any pressure effects.

### *3.5. Microhardness*

A Vickers hardness of ~350HV was established for pre-heat treated parts, with an increase to ~500HV after heat treatment, remaining consistent across all three production batches, and consistent with other reported results [21]. These baseline measurements were conducted to facilitate further research into surface finishing techniques, such as anodising and electro-polishing, to quantify any effect on hardness.

### *3.6. Porosity*

A representative cross-sectional image of one of the e-manufactured components is given in Fig. 5. The areal density of porosity was measured to be 0.28±0.05 %, comparable with the expected range of porosity present in an ALM processed Titanium alloy, using manufacturers parameters (>99% density) [21, 23].

Fig. 5. Optical micrograph of a sample of EOS Titanium 64.

## 4. Conclusions

The mechanical integrity of thin walled (0.5mm) hydraulic channels produced by DMLS have been tested against the conditions found in a demanding real world motorsports application, demonstrating their robust capabilities and the consistency of components manufactured by this route. The ability to produce dimensionally accurate components, with appropriate hardness was also demonstrated. This will provide end-users confidence in the capability of DMLS technology to provide mechanical and geometrical properties that match those obtained through traditional manufacturing processes. A potential requirement for surface post-treatment has been indicated, and end-users must appreciate this, and if necessary, apply appropriate surface treatment techniques to satisfy their application needs.

The work outlined exhibits not only the mechanical integrity of components produced by DMLS, but the functional benefits which accompany the use of this technology in an engineering design context. The ability to create free form geometry provides the potential to enhance the performance of complex components, not only by reducing component weight, but by improving functionality with the potential for more efficient fluid flow (up to 250%). This is particularly applicable in a motorsport context, with small production batches of components which undergo repeated re-design in the search of further performance benefits.

Thus DMLS has the capability to provide mechanically capable, geometrically accurate components, which, combined with the ability to introduce internal geometrical complexity, offers significant opportunity for end-users to enhance performance of components and systems. The onus is now on designers to embrace this capability and be innovative in their design processes to extract the maximum potential of this exciting new manufacturing capability.

**Acknowledgements**

The authors would like to express their thanks to all those at Red Bull Technology (for whom the project which led to this paper was undertaken) for their invaluable assistance and insight, and our gratitude for the significant support provided by the EOS group. Also our thanks to Index Instruments for the provision of their REF 804 hand held Refractometer and to IMCD UK Ltd for supply of Silicone Oil used. Thanks also to Joe Nawasra at the University of Warwick Optical Engineering Laboratory for the use of their facilities and advice. Thanks also to WMG for provision of facilities and funding.

## References

1. FIA (2012) *2012 Formula One Technical Regulations*.
2. Li, C.H., Z. Fang, and H.Y. Zhao. *Investigation into Layered Manufacturing Technologies for Industrial Applications*. in *2010 Second International Conference on Multimedia and Information Technology (MMIT 2010), 24-25 April 2010*. 2010. Los Alamitos, CA, USA: IEEE Computer Society.
3. Kai CC, F.L., *Rapid Prototyping, Principles and Applications in Manufacturing*. 1997, Singapore: World Scientific Publishing Co.Pte. Ltd.
4. Matthews, C., *Engineers' Data Book, Third Edition*. 2006, Chichester: John Wiley and Sons.
5. Rochus, P., et al., *New applications of rapid prototyping and rapid manufacturing (RP/RM) technologies for space instrumentation.* Acta Astronautica, 2007. **61**(1-6): p. 352-359.
6. Hanninen, J., *DMLS moves from rapid tooling to rapid manufacturing.* Metal Powder Report, 2001. **56**(9): p. 24-26.
7. Santos, E.C., et al., *Rapid manufacturing of metal components by laser forming.* International Journal of Machine Tools and Manufacture, 2006. **46**(12-13): p. 1459-1468.
8. Hopkinson, N.H., RJM. Dickens, PM., *Rapid Manufacturing, an Industrial Revolution for the Digital Age*. 2006, Cheshire: John Wiley & Sons.
9. Sedacca, B., *Hand built by lasers [additive layer manufacturing].* Engineering & Technology, 2011. **6**(Copyright 2011, The Institution of Engineering and Technology): p. 58-60.
10. BS EN 2624:2007. Aerospace series - Pressure impulse testing of hydraulic system components, BSi 2007.
11. Udrea, D.D., et al. *Application of PIV (particle image velocimetry) and flow visualization to the coolant flow through an automotive engine*. in *New Image Processing Techniques and Applications: Algorithms, Methods, and Components II, 18-19 June 1997*. 1997. USA: SPIE-Int. Soc. Opt. Eng.
12. Reeves, M., et al., *A high-speed all-digital technique for cycle-resolved 2-D flow measurement and flow visualisation within SI engine cylinders.* Optics and Lasers in Engineering, 1999. **31**(4): p. 247-261.
13. DSM-Desotech. *Watershed XC11122 Datasheet*. 2009; Available from: http://www.dsm.com/en_US/downloads/11122_Data_Sheet2.pdf.
14. LaVision-GmbH, *DaVis FlowMaster Software Manual for DaVis 7.0.* 2005.
15. BS EN ISO 25178-602:2010 Part 603. Geometrical product specifications (GPS) - Surface texture: Areal, BSi 2010.
16. BS EN ISO 10360-5:2010. Geometrical product specifications (GPS) - Acceptance and reverification tests for coordinate measuring machines, BSi 2010.

17. BS EN ISO 14577-1:2002. Metallic materials - Instrumented indentation test for hardness and materials parameters - Part 1: Test method, BSi 2002.
18. ASTM E2109 - 01(2007). Test Methods for Determining Area Percentage Porosity in Thermal Sprayed Coatings, ASTM 2007.
19. Petrovic, V., et al., *Additive layered manufacturing: sectors of industrial application shown through case studies.* International Journal of Production Research, 2011. **49**(Copyright 2011, The Institution of Engineering and Technology): p. 1061-79.
20. Levy, G.N., R. Schindel, and J.P. Kruth, *RAPID MANUFACTURING AND RAPID TOOLING WITH LAYER MANUFACTURING (LM) TECHNOLOGIES, STATE OF THE ART AND FUTURE PERSPECTIVES.* CIRP Annals - Manufacturing Technology, 2003. **52**(2): p. 589-609.
21. Bertol, L.S., et al., *Medical design: Direct metal laser sintering of Ti–6Al–4V.* Materials & Design, 2010. **31**(8): p. 3982-3988.
22. Ning, Y., et al., *An approach to minimize build errors in direct metal laser sintering.* IEEE Transactions on Automation Science and Engineering, 2006. **3**(1): p. 73-80.
23. Thijs, L., et al., *A study of the micro structural evolution during selective laser melting of Ti-6Al-4V.* Acta Materialia, 2010. **58**(9): p. 3303-3312.

## Tables & Figures

Fig. 1. DMLS parts both pre (a) and post (b) machined.

Fig. 2. Pressure test rig, twin walled safety enclosure, pressure sensor & valve.

Fig. 3. Vector fields and test samples for traditional and AM geometry 1.

Fig. 4. Vector fields and test samples for traditional and AM geometry 2.

Fig. 5. Optical micrograph of a sample of EOS Titanium 64.

Table. 1. Fluid flow measurements for traditional and e-manufactured geometries at centre and end points of the flow path.

Table. 2. Surface roughness measurements for the DMLS samples.

Table. 3. Torsional and axial alignments for the DMLS samples.

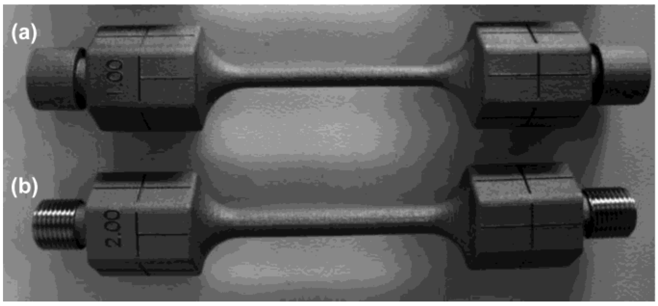
(a)
(b)
1.00
2.00

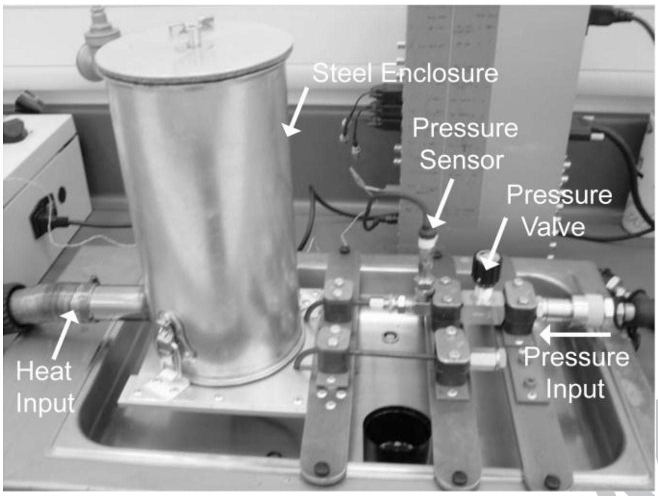
Steel Enclosure
Pressure Sensor
Pressure Valve
Heat Input
Pressure Input

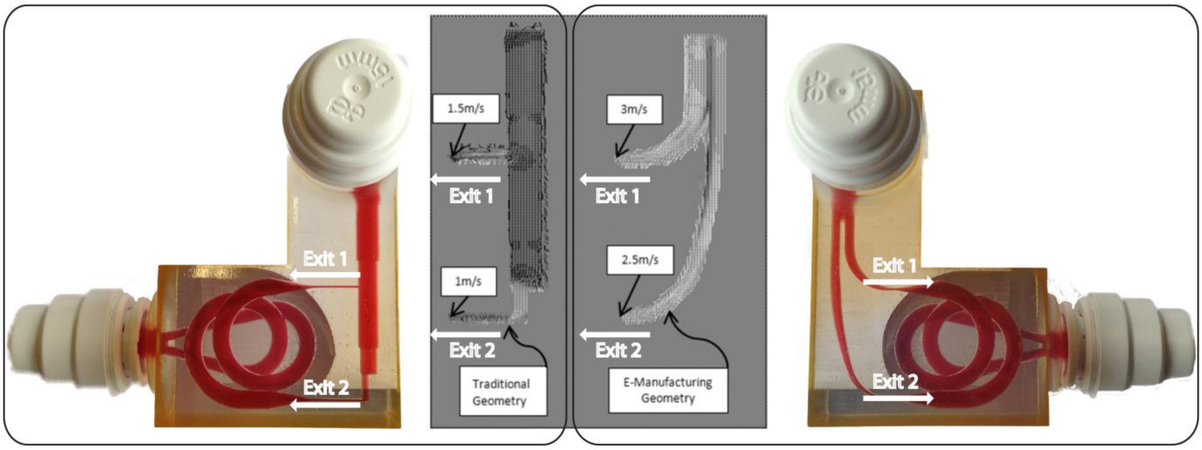
Exit 1
Exit 2
1.5m/s
1m/s
Exit 1
Exit 2
Traditional Geometry
3m/s
2.5m/s
Exit 1
Exit 2
E-Manufacturing Geometry
Exit 1
Exit 2

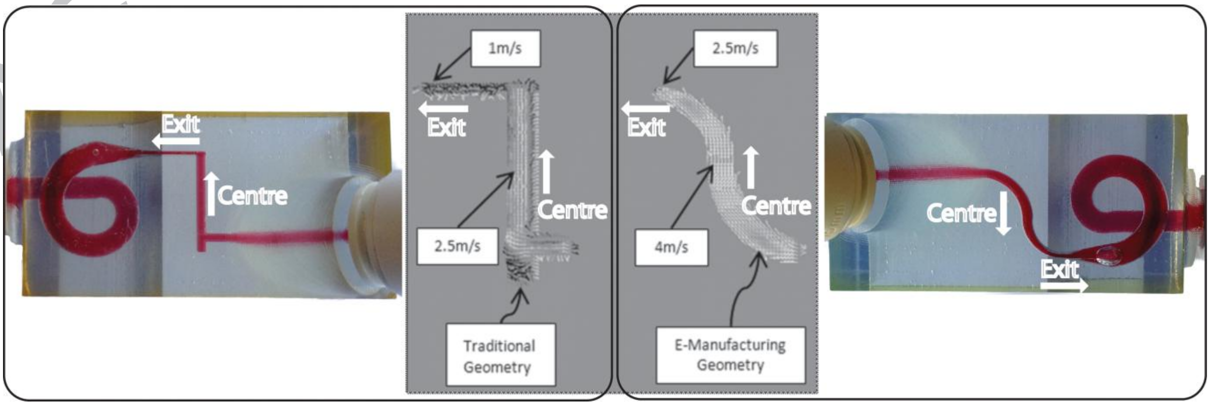
Exit
Centre
1m/s
Exit
Centre
2.5m/s
Traditional Geometry
2.5m/s
Exit
Centre
4m/s
E-Manufacturing Geometry
Centre
Exit

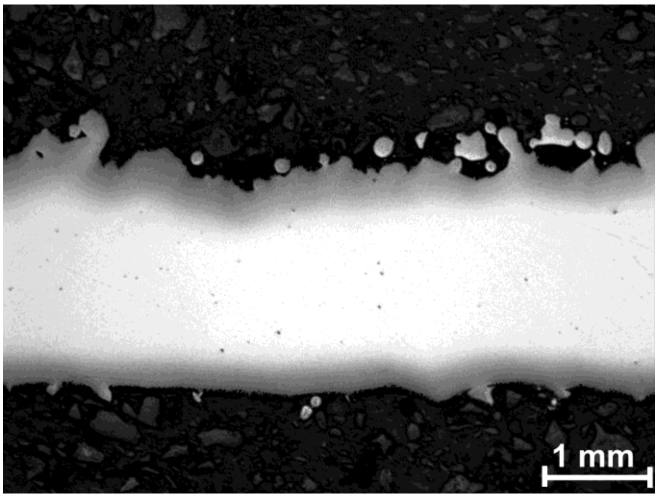


| Sample | Traditional (m/s) | AM (m/s) | [Δ%] |
|---|---|---|---|
| Fig 3, exit | 1.5 | 3.0 | 100 |
| Fig 3, exit | 1.0 | 2.5 | 250 |
| Fig 4, centre | 2.5 | 4.0 | 160 |
| Fig 4, exit | 1.0 | 2.5 | 250 |

| Position | $R_a$ (μm) |
|---|---|
| Top surface | 3.96±0.05 |
| Upper facing sloping surface | 8.95±0.05 |
| Lower facing sloping surface | 17.50±0.05 |
| Supported surface | 27.93±0.05 |

| Sample | Torsional Alignment (°±0.5) | | | Axial Alignment (°±0.5) | | |
|---|---|---|---|---|---|---|
| | Pre | Post | [Δ] | Pre | Post | [Δ] |
| 0.5Tube | 1.14 | 1.31 | 0.17 | 0.82 | 1.07 | 0.25 |
| 0.65Tube | 0.69 | 0.94 | 0.25 | 0.7 | 0.68 | 0.02 |
| 0.85Tube | 0.98 | 0.77 | 0.21 | 0.52 | 1.35 | 0.83 |
| 1.00 Tube | 0.34 | 1.07 | 0.73 | 0.39 | 0.44 | 0.05 |
| 1.25Tube | 0.34 | 0.58 | 0.24 | 0.12 | 1.56 | 1.44 |
| 1.50Tube | 0.23 | 0.75 | 0.52 | 0.05 | 0.33 | 0.28 |
| 1.75Tube | 0.49 | 0.37 | 0.12 | 0.13 | 0.28 | 0.15 |
| 2.00Tube | 0.24 | 0.79 | 0.55 | 0.21 | 0.12 | 0.09 |
| 0.5Ellipse | 1.64 | 2.33 | 0.69 | 1.19 | 0.81 | 0.38 |
| 0.5Hexagonal | 0.98 | 2.38 | 1.40 | 0.12 | 0.53 | 0.41 |

Table 1



| Sample | Traditional (m/s) | AM (m/s) | [Δ%] |
|---|---|---|---|
| Fig 3, exit1 | 1.5 | 3.0 | 100 |
| Fig 3, exit2 | 1.0 | 2.5 | 250 |
| Fig 4, centre | 2.5 | 4.0 | 160 |
| Fig 4, exit | 1.0 | 2.5 | 250 |

Table 2



| **Position** | **$R_a$ (μm)** |
|---|---|
| Top surface | 3.96±0.05 |
| Upper facing sloping surface | 8.95±0.05 |
| Lower facing sloping surface | 17.50±0.05 |
| Supported surface | 27.93±0.05 |

Table 3



| **Sample** | **Torsional Alignment (°±0.5)** | | | **Axial Alignment (°±0.5)** | | |
|---|---|---|---|---|---|---|
| | Pre | Post | [Δ] | Pre | Post | [Δ] |
| 0.5Tube | 1.14 | 1.31 | 0.17 | 0.82 | 1.07 | 0.25 |
| 0.65Tube | 0.69 | 0.94 | 0.25 | 0.7 | 0.68 | 0.02 |
| 0.85Tube | 0.98 | 0.77 | 0.21 | 0.52 | 1.35 | 0.83 |
| 1.00 Tube | 0.34 | 1.07 | 0.73 | 0.39 | 0.44 | 0.05 |
| 1.25Tube | 0.34 | 0.58 | 0.24 | 0.12 | 1.56 | 1.44 |
| 1.50Tube | 0.23 | 0.75 | 0.52 | 0.05 | 0.33 | 0.28 |
| 1.75Tube | 0.49 | 0.37 | 0.12 | 0.13 | 0.28 | 0.15 |
| 2.00Tube | 0.24 | 0.79 | 0.55 | 0.21 | 0.12 | 0.09 |
| 0.5Ellipse | 1.64 | 2.33 | 0.69 | 1.19 | 0.81 | 0.38 |
| 0.5Hexagonal | 0.98 | 2.38 | 1.40 | 0.12 | 0.53 | 0.41 |

Figure 1



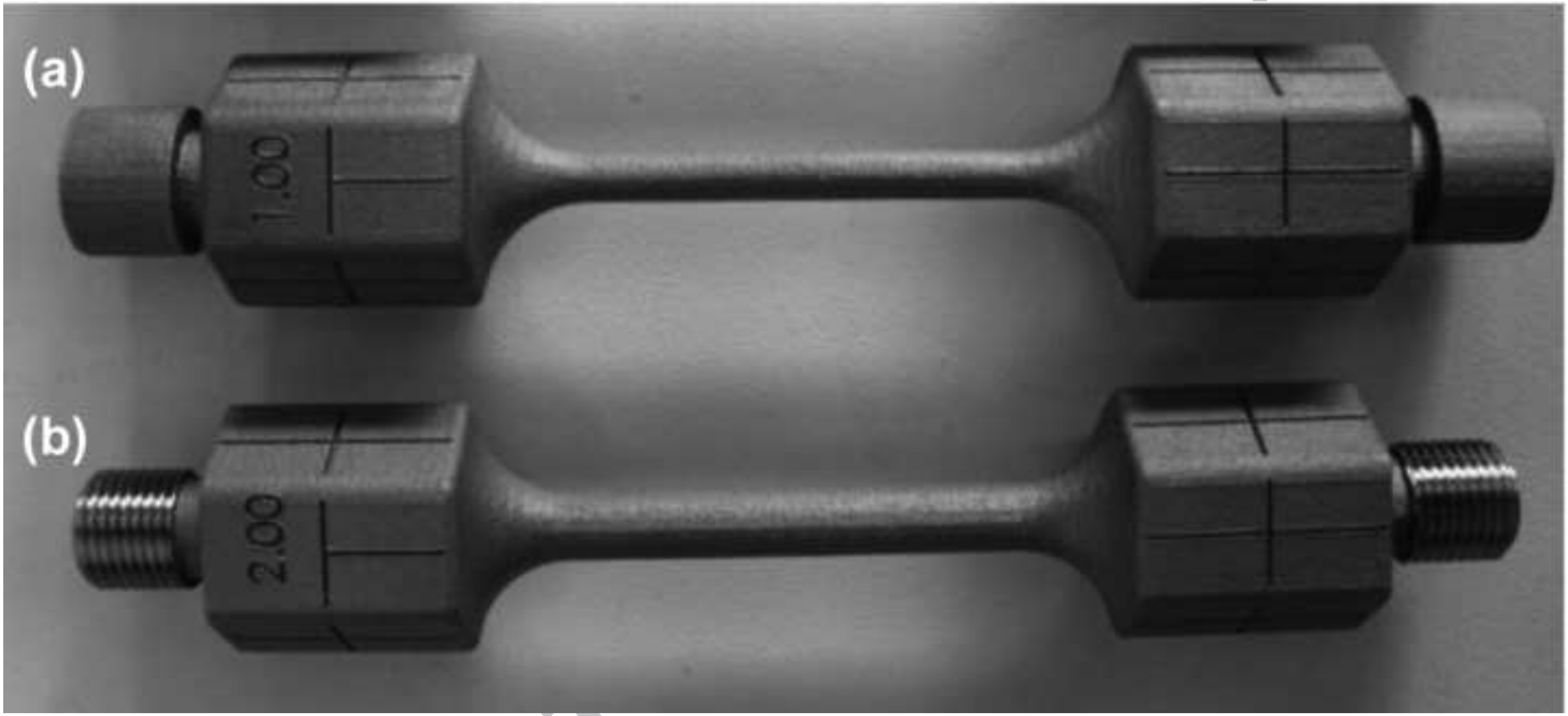

Figure 2



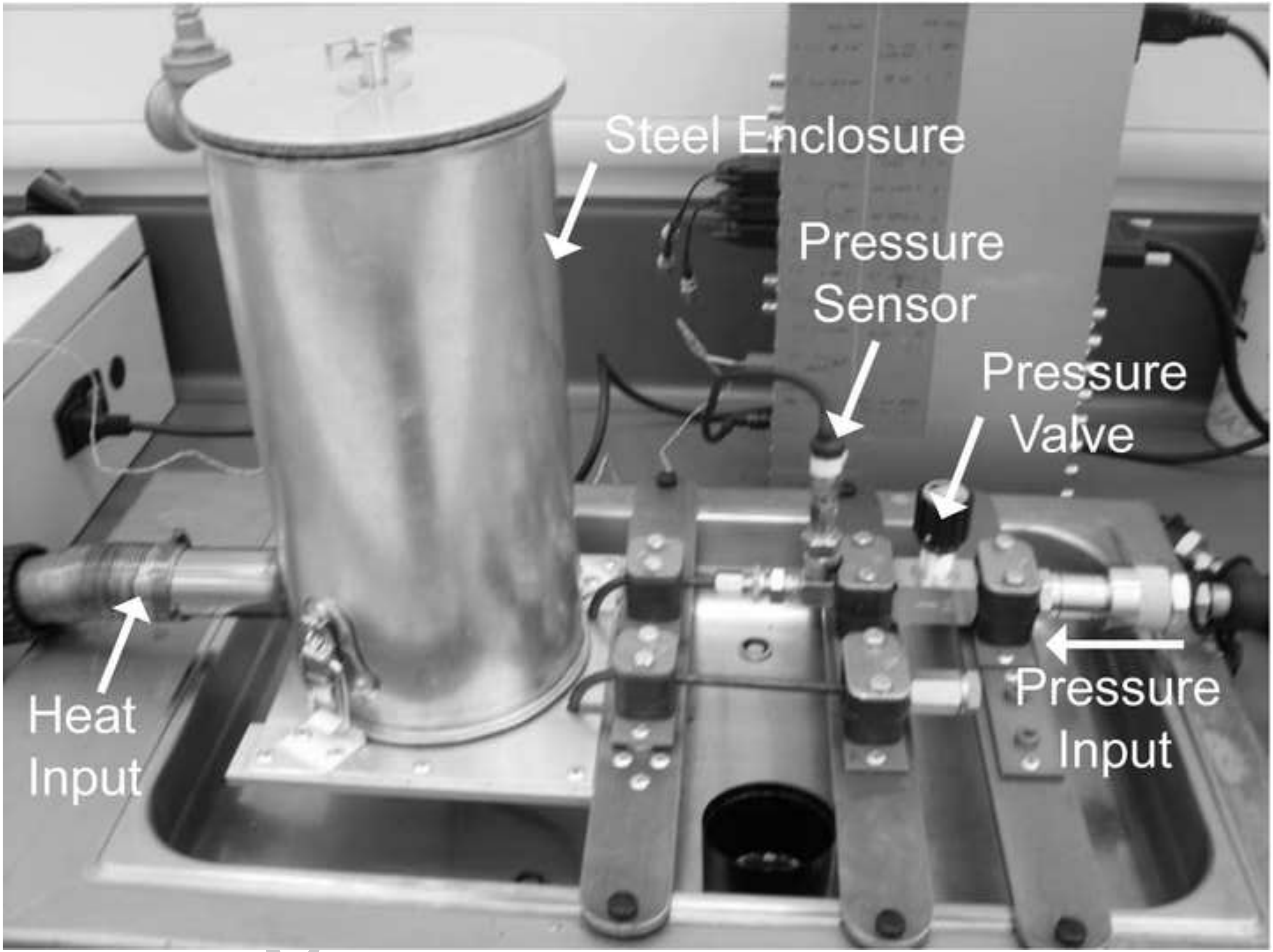
Steel Enclosure
Pressure Sensor
Pressure Valve
Heat Input
Pressure Input

Figure 3



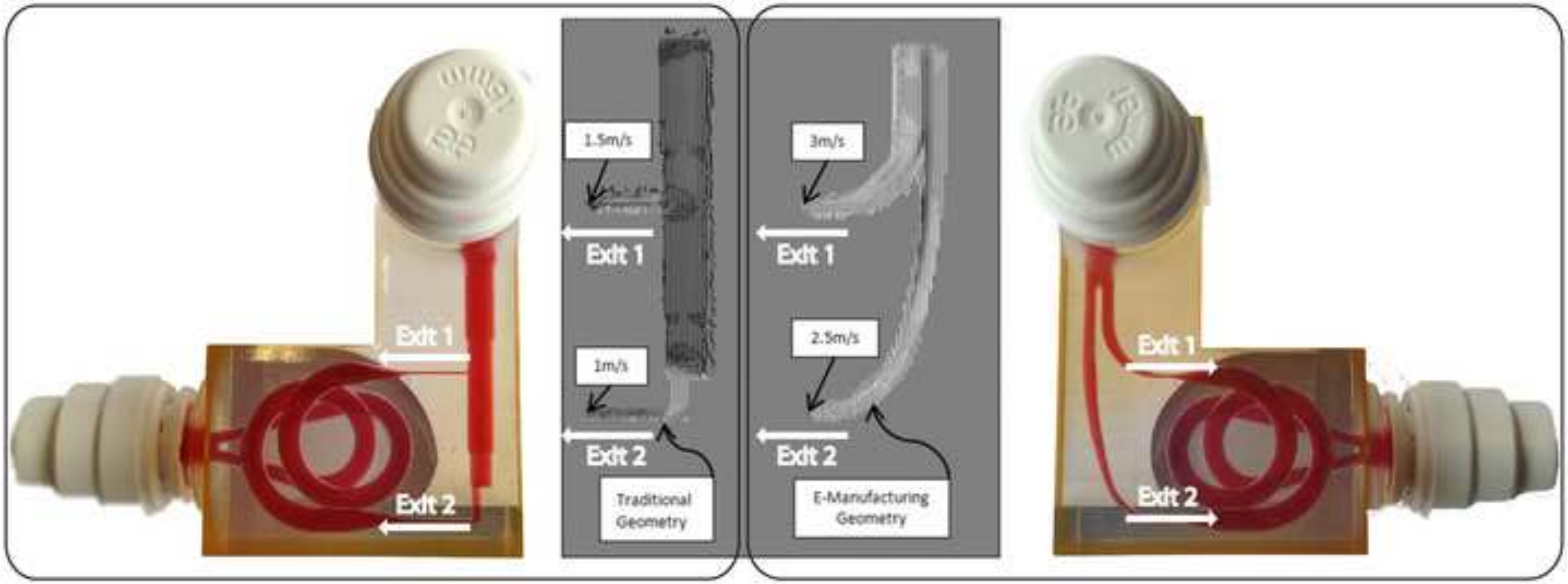
Exit 1
Exit 2
1.5m/s
1m/s
Exit 1
Exit 2
Traditional Geometry
3m/s
2.5m/s
Exit 1
Exit 2
E-Manufacturing Geometry
Exit 1
Exit 2

Figure 4



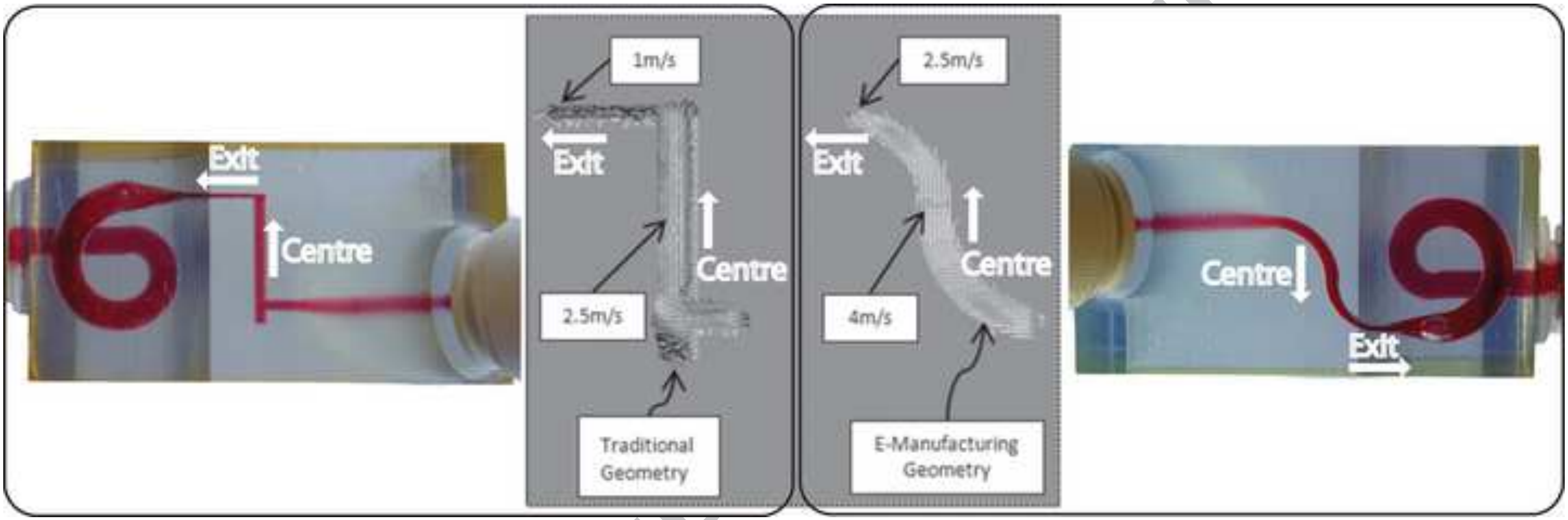

Exit
Centre
1m/s
Exit
Centre
2.5m/s
Traditional Geometry
2.5m/s
Exit
Centre
4m/s
E-Manufacturing Geometry
Centre
Exit

Figure 5



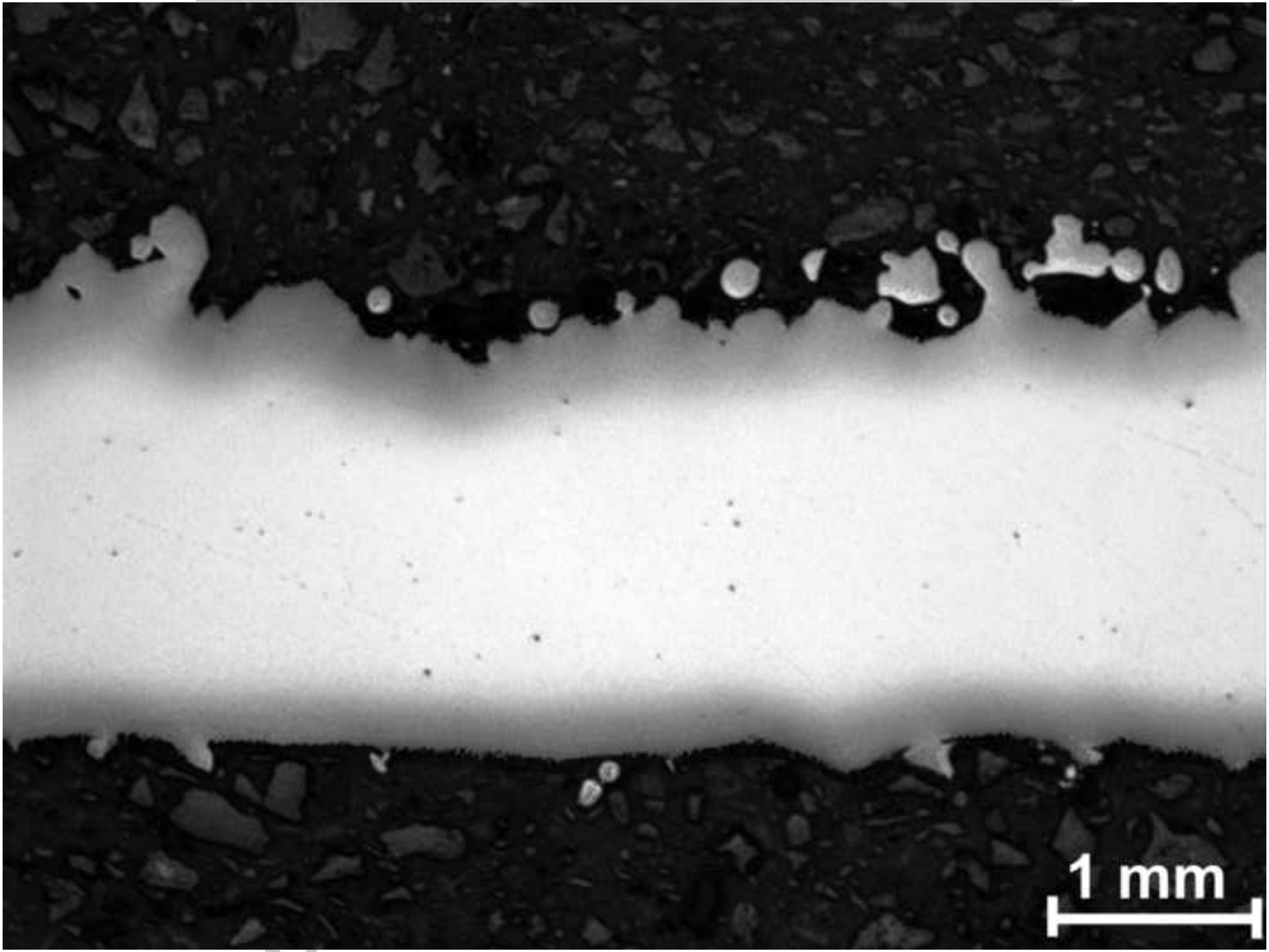

**Highlights**

Additive Manufacturing in a high value manufacturing application evaluated.

Geometric design freedom produced flow passages with 250% velocity increase.

Laser melted Ti64 flow passages with 0.5mm wall validated for pneumatic manifolds.